Available online at www.sciencedirect.com
ScienceDirect
Chemical Geology 246 (2007) 87–106
CHEMICAL GEOLOGY
INCLUDING
ISOTOPE GEOSCIENCE
www.elsevier.com/locate/chemgeo

Active venting at the Isis mud volcano, offshore Egypt: Origin and migration of hydrocarbons

Vincent Mastalerz [a,*], Gert J. de Lange [a], Anke Dählmann [a], Tomas Feseker [b]

[a] *Utrecht University, Faculty of Geosciences, Department of Earth Sciences – Geochemistry, P.O. Box 80021, 3508 TA Utrecht, The Netherlands*
[b] *Ifremer, Géosciences Marines, B.P. 70, 29280 Plouzané, France*

Received 9 February 2007; received in revised form 12 September 2007; accepted 14 September 2007

Editor: D. Rickard

Abstract

The Isis mud volcano is an active camembert-like mud expulsion structure in the eastern Nile deep-sea fan area. It has been investigated during the NAUTINIL (2003) and MIMES (2004) cruises carried out within the MEDIFLUX project. Active, gas-rich fluid venting occurs at the Isis mud volcano as indicated by enhanced gas content in the sediments, having a measured 7.5 mmol of methane per liter of wet sediment in the central area of the mud volcano. In addition, gas bubble expulsions have resulted in the formation of multiple hydrocarbon plumes in the water column, with methane concentrations as high as 1550 nmol/L, compared to ~1 nmol/L for background levels in deep water.

In view of the stable carbon and hydrogen isotopic composition of methane ($\delta^{13}C = -55.1‰$ VPDB, $\delta D = -203‰$ VSMOW) and of higher hydrocarbons ($\delta^{13}C$ of −30.3‰, −26.1‰, −28.4‰, and −25.0‰ VPDB, for ethane, propane, *i*-butane and *n*-butane, respectively), their origin is mainly thermogenic. These isotopic data also show that the wet compounds are co-generated with oil and we suggest they predominantly originate from type II kerogen source rocks of potentially variable maturity levels.

At the centre of the mud volcano, the distinct kink observed in the pore water isotopic and dissolved species composition and its depth level change between subsequent cruises indicates a high frequency of fluid/gas expulsion. The seawater signature of the pore fluid in the upper part of the sediment column suggests that each expulsion is followed by a downward migration of overlying seawater. Such downward advection of bottom seawater may not only be related to the replacement of the ejected gas but also to the replacement of lower density pore fluid by bottom seawater. This mechanism is thought to be a common feature at mud volcanoes and gas seepage sites.

In the peripheral zone, pore fluid is at seawater concentration and isotopic composition, down to a coring depth of 430 cmbsf. We suggest that the deeper downward advection of bottom seawater is related to the less frequent fluid/gas expulsion occurring at these sites compared to the centre sites.

In this paper we show that a combination of geochemical tools used for hydrocarbons and pore water geochemistry is a powerful approach to detect sources of ascending fluid and to reveal post-eruptional fluidodynamic processes within mud volcanoes.

Keywords: Mud volcano; Nile deep-sea fan; Methane; Hydrocarbons; Stable isotope; Downward advection

1. Introduction

Gas seepages and related geological structures have been found worldwide. Mud volcanoes (MVs) are the largest examples of seepage-related geomorphological

* Corresponding author. Tel.: +31 30 253 4991; fax: +31 253 5302.
E-mail address: v.mastalerz@geo.uu.nl (V. Mastalerz).

0009-2541/$ - see front matter © 2007 Elsevier B.V. All rights reserved.
doi:10.1016/j.chemgeo.2007.09.005

features occurring at the seafloor within active continental margins such as the Makran accretionary wedge off Pakistan (von Rad et al., 2000), the Cascadian margin (Suess et al., 1999), the Aleutian subduction zone (Suess et al., 1998), the Costa Rica forearc (Schmidt et al., 2005), the Okhotsk Sea (Gaedicke et al., 1997; Shakirov et al., 2004; Obzhirov et al., 2004) and within passive margins where high sediment rates occur, such as in the Gulf of Mexico (Sassen et al., 1999), the Niger delta (Hovland et al., 1997), the Eel River Basin (Burger et al., 2001). In the eastern Mediterranean, mud expulsion structures occur at the Mediterranean Ridge due to the collision between the African and Eurasian tectonic plates (Camerlenghi et al., 1995; Cita et al., 1996; Kopf and Behrmann, 2000), in the Anaximander area (Woodside et al., 1998; Zitter, 2004) and were recently documented in the Nile deep-sea fan (Mascle et al., 2001; Loncke, 2002; Loncke et al., 2004). Fluid venting area and related MV provinces are important geological settings for hydrocarbons gas release into the overlying water column (Judd et al., 2002; Dimitrov, 2002, 2003; Mazurenko and Soloviev, 2003). The formation of MVs is the result of a catastrophic expulsion of an overpressurised complex mixture of sediment, water, and various chemicals where hydrocarbon gases (mainly methane) and in some cases petroleum are the dominant components. Thus the presence of seepage indicates the existence of subsurface accumulations of hydrocarbons and migration pathways. In this study, we present a comprehensive geochemical investigation of pore water and water column hydrocarbon data at the Isis MV, a mud structure located in the eastern part of the Nile deep-sea fan. The aims of this work are: (1) to investigate the composition and the origin of the light gaseous hydrocarbons in sediments and water column; and (2) to identify and to assess the potential processes at such mud expulsion structure.

2. Geological background

The Isis MV is located in the eastern part of the Nile deep-sea fan at the water depth of about 991 m water depth, in the eastern part of the Nile fan and has a camembert-like morphology with a circular plateau of about 4.2 km in diameter that is elevated ~50 m above the surrounding seafloor (Fig. 1; Loncke, 2002; Loncke et al., 2004). The Isis MV is clearly emplaced outside of the Messinian (Late Miocene) evaporite zone and sited at an active fault system which can act as conduits for migrating fluids (Loncke et al., 2004). Details on the tectonic background of this region have been published elsewhere (Mascle et al., 2001; Loncke, 2002; Loncke et al., 2004).

3. Origin of hydrocarbon gases and processes affecting their molecular and isotopic compositions

The origin of gases and the processes that may affect their initial composition can be assessed using the relative abundance of higher hydrocarbons, the isotopic composition of methane and of higher hydrocarbons, and the vitrinite reflectance. We briefly introduce each of these approaches, which will subsequently be applied in the discussion.

3.1. Relative abundance of higher hydrocarbons

Methane is the most abundant hydrocarbon gas on Earth (Schoell, 1980). At MVs and gas seepages methane is associated with pore fluids and originates from either microbial or thermal degradation of organic matter (primary cracking) and from oil and gas heating (secondary cracking) (Hunt, 1996). Heavier hydrocarbons, i.e. C_{2+}, originate generally from thermal cracking reactions (Cline and Holmes, 1977; Sandstrom et al., 1983; Pepper and Corvi, 1995) and their proportion increases with the maturation of the source rock. Hence, the relative proportion of gaseous hydrocarbons can provide an initial classification of a gas type using molecular ratio such as the wetness ratio $(C_{2+}/(C_1+C_{2+})\times 100$, with $C_{2+}=\sum C^{i}_{2-6}$ Schoell, 1983). Accordingly, "dry" gases have a wetness ratio lower than 1% and are derived from microbial activity and/or from low mature or overmature source rock. "Wet" gases are thermally derived and have a wetness ratio higher than 5%. Gases with a wetness ratio between 1 and 5% are considered to be a mixture of both biogenic and thermal origin (Schoell, 1988). Abiogenic formation of alkanes is a third potential formation mechanism occurring during magma cooling or in hydrothermal systems. The latter mechanism is not applicable here (Sherwood Lollar et al., 2002).

3.2. Isotopic composition of hydrocarbons

The stable carbon and hydrogen isotopic composition of methane has also been extensively used to determine whether methane has been microbially or thermally produced (Stahl, 1977, 1979; Schoell, 1980; Chung et al., 1988; Katz et al., 2002). Typical $\delta^{13}C_1$ values range from −110‰ to −50‰ VPDB for biogenic gas and from −50‰ to −20‰ VSMOW for thermogenic gas. The δD values are less indicative and extend from −350‰ to −150‰ VSMOW for biogenic gas and from −300‰ to −90‰ VSMOW for thermogenic gas.

After formation, hydrocarbons migrate from source rock towards a reservoir where they accumulate. Post-

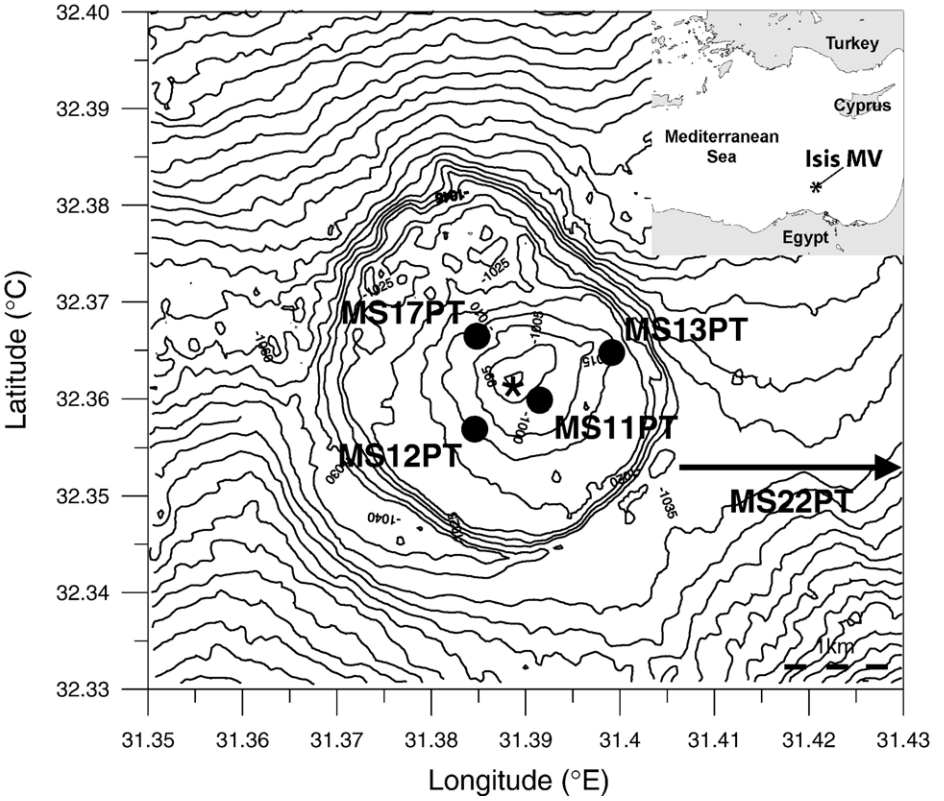

Fig. 1. Location of the Isis mud volcano, Nile deep-sea fan, eastern Mediterranean, with the positions of the sampling stations. The asterisk indicates the sampling locations of cores and CTD at the centre of the MV (NLK06F, MS24PT, MS19GT, MS09PC, NLCTD6, and MS23CT). The filled symbols indicate the sampling locations of the off-centre cores (MS11PT, MS12PT, MS13PT, and MS17PT). Reference core MS22PT is well outside the mud volcano and appears at the east side of the map as indicated by the large arrow. (Map courtesy of H. Ondréas).

genetic processes such as source mixing (Prinzhofer and Pernaton, 1997), biodegradation (Zhang and Krooss, 2001) and fractionation during diffusive way of migration (Fuex, 1980; Zhang and Krooss, 2001; Lückge et al., 2002) can affect the carbon and hydrogen isotopic composition of methane and can thus lead to a misinterpretation of its origin. Moreover, since heavier hydrocarbons are not subject to diffusive fractionation (Chung et al., 1988; Berner and Faber, 1996), their isotopic composition is a more reliable indicator of the gas source although biodegradation of wet gaseous components was also detected (James and Burns, 1984, Clayton et al., 1997; Pallasser, 2000). Chung et al. (1988) proposed a model to investigate the extent of gas mixing and/or biodegradation. The various hydrocarbons released during source rock cracking are controlled by a kinetic isotope effect. Since the $^{12}C–^{12}C$ bond breaks easier than the $^{12}C–^{13}C$ bond, the hydrocarbon products are isotopically lighter than the source rock. This process is reflected by a linear relation between the inverse carbon number of the hydrocarbons ($1/n$) and their carbon isotopic composition. By extrapolating the line to the $1/n=1$ (i.e. methane), this so-called "natural gas plot model" permits the estimate of the carbon isotopic signature for the thermogenic methane end-member and thus the appraisal of the occurrence of biodegradation. If thermally derived methane mixes with microbially produced methane, the $\delta^{13}C_1$ value deviates from this linearity. In that case, one can use the gas plot model to calculate the biogenic contribution to the gas mixture applying a mixing model.

3.3. Vitrinite reflectance

The vitrinite reflectance ($\%R_o$) is a common parameter used to characterize the maturity level of the gas source kerogen. It increases with maturity and ranges from 0.5% (early mature) to 3% (late mature). We will use two models that relate isotopic composition of hydrocarbons to maturity levels.

Berner and Faber (1996) developed an empirical model that plots the maturity curve on a $\delta^{13}C_2$ versus

$\delta^{13}C_3$ diagram. The strong point of this model is that the maturity curve is a function of the nature of the source rock (type II, i.e. related to marine organic matter, or type III, i.e. related to organic matter derived from terrestrial plants) and of its $\delta^{13}C$ value (Appendix A, Eqs. (A.1)–(A.4), Fig. 9B).

Lorant et al. (1998) proposed an alternative method to assess maturity, namely from a diagram plotting the C_2/C_3 ratio versus the $\delta^{13}C_2-\delta^{13}C_3$ difference (Fig. 9A). Their model is based on the fact that isotopic fractionation of hydrocarbons is not mainly controlled by the maturity level, but rather by the residence time of generated gases before their expulsion towards the reservoir. A short residence time leads to the expulsion of early mature gas, whereas, a longer residence time leads to mature gases that may undergo additional thermo-cracking. The diagram thus defines the different areas of gas genesis, especially the primary and the secondary cracking zones.

All of the above approaches will be used here to assess the origin for hydrocarbons at the Isis MV.

4. Materials and methods

Water and sediment columns at the Isis MV were sampled during the NAUTINIL cruise in September/October 2003 with R/V *Atalante* (stations labelled NL) and MIMES cruise in June/July 2004 with R/V *Pelagia* (stations labelled MS). During NAUTINIL, one CTD cast and one sediment core (stations NLCTD6 and NLK06F, respectively; Table 1, Fig. 1) were taken at the centre of the MV. During MIMES, one CTD cast (station MS23CT), three cores at the centre (stations MS09PC, MS19GT, and MS24PT), and four cores off-centre (stations MS11PT, MS12PT, MS13PT, and MS17PT) have been taken (Table 1, Fig. 1). An additional reference core was taken outside the MV (station MS22PT; Table 1, Fig. 1).

Table 1
Positions of the sampling stations at Isis MV during the NAUTINIL and MIMES cruises

Station	Sampling device	Latitude (°N)	Longitude (°E)
NAUTINIL 2003 cruise			
Centre			
NLCTD6	CTD	32.36110	31.38946
NLK06F	Piston core	32.36110	31.38946
MIMES 2004 cruise			
Centre			
MS23CT	CTD	32.36091	31.38956
MS24PT	Piston core	32.36098	31.38952
MS19GT	Gravity core	32.36097	31.38952
MS09PC	Piston core	32.36092	31.38958
Off-centre			
MS11PT	Piston core	32.35987	31.39148
MS12PT	Piston core	32.35690	31.38460
MS13PT	Piston core	32.36477	31.39912
MS17PT	Piston core	32.36645	31.38483
Reference			
MS22PT	Piston core	32.35670	31.44502

The Isis MV was also explored with the French submersible *Nautile* in 2003. A total of three dives were carried out, among which two explored the volcano on transects from SE to NW and from NE to SW, and one focused on the centre of the structure.

4.1. Water sampling

Sampling of the water column took place with a CTD rosette sampler equipped with 15 Niskin bottles during NAUTINIL and with 22 NOEX bottles (NO Exchange, http://www.technicap.com) during MIMES. In the latter cruise, the R/V *Pelagia* remained within 30 m "on site" during the CTD cast. The bottles were collected during the ascend of the CTD rosette and the first two bottles were closed at the same depth after the CTD rosette became stationary 6 m above the seafloor. The remaining CTD bottles were closed after waiting for 1 min at each depth level.

For hydrocarbon gas compositional and stable isotope analysis, water sub-samples were taken immediately upon arrival of the CTD rosette sampler on deck. Schott bottles (250 mL) were filled air bubble free and quickly sealed with a gas-tight butyl stopper. About 100 μL of mercuric chloride ($HgCl_2$ solution, 70 g/L) was added to stop any biogenic activity. A headspace of 10 mL was made with nitrogen gas (purity 5.0) while simultaneously removing 10 mL of the sample using a second needle. The samples were equilibrated upside down for at least 24 h at room temperature prior to measurement and were kept upside down until on shore analyses for isotopic composition.

4.2. Sediment sampling

4.2.1. Hydrocarbon gases

For gas analysis, 3 mL (NAUTINIL) and 10 mL (MIMES) of sediment samples were taken immediately after core retrieval with a cut syringe. The sediment was put into a 30-mL (NAUTINIL) and a 65-mL (MIMES) glass bottle pre-filled with saturated NaCl solution (ca. 300 g/L) that was quickly sealed with a gas-tight butyl stopper, allowing no air to remain in the bottle. A headspace of 5 mL was made with nitrogen gas (purity 5.0) gas while simultaneously removing 5 mL of salt-water using a second needle. The bottles were shaken to

make a homogeneous suspension and equilibrated upside down for 24 h at room temperature prior to gas analysis. During the MIMES cruise, duplicate sediment samples were taken for onshore stable isotope analysis, using the same procedure only making a 10-mL headspace.

4.2.2. Pore waters

Pore waters were extracted from 20–40 mL of sediment by centrifugation or squeezing (de Lange, 1992). Pore water was then filtered through a 0.2-μm cellulose-acetate membrane. For major element analyses, 4-mL sub-samples were acidified with 100 μL of suprapure HNO_3 acid (1 M). For dissolved inorganic carbon (DIC) and nutrients, sub-samples were stored in 4-mL glass vials. All sub-samples were stored in the dark at 4 °C.

4.3. Analytical procedures

4.3.1. Hydrocarbon gas concentrations

During the NAUTINIL cruise, methane concentrations were determined on board, injecting 1-mL gas sample into a Shimadzu gas chromatograph (GC) GC-14B with a FID (Flame Ionization Detector) and equipped with a packed stainless steel Porapack Q (6 ft, 2 mm i.d., 80/100 mesh, Alltech). The oven was kept at 30 °C. The heavier hydrocarbons were analyzed onshore with a Trace GC equipped with a 32-m-long HP-PLOT capillary column (10 μm). The GC oven was held at 40 °C for 3 min, ramped to 185 °C at 20 °C/min and finally held constant for 8 min.

During the MIMES cruise, the Shimadzu GC GC-14B has been equipped with a 0.25-mL sample loop and a Valco-plot-HayeSep D capillary column (30 m × 0.53 mm i.d. × 20 μm). At least 10 mL of nitrogen was used to flush the sample loop prior to each sample. The GC oven was held at 60 °C for 2 min, raised to 180 °C at 35 °C/min and finally held constant for 8 min.

The following standards were measured three times prior to the analysis of a set of samples: 15, 100, and 1000 ppmv C_1–C_6 mixture, 1000 ppmv methane and 1% methane (all from Scotty). The precision of the method is around 3%. The concentration of each gas component in the headspace was calculated off-line from the peak area. The concentration of each component in the liquid phase was calculated from the headspace concentration using the Bunsen solubility coefficient β (Grasshoff et al., 1983).

Due to the large oversaturation of gases in most of the studied sediment samples, a substantial but unknown amount of gas may have escaped during core retrieval and on-deck handling. The measured concentrations for sediment samples are therefore minimum values.

All concentrations are corrected for volume, salinity, and temperature and then reported in nmol/L for the water samples and in μmol/L of wet sediment for the sediment samples.

4.3.2. Stable carbon and hydrogen isotopes of hydrocarbons and CO_2

The MIMES sediment samples were analyzed for hydrocarbon and CO_2 isotopes at Utrecht University using a Gas Chromatograph–Isotope Ratio Mass Spectrometer (GC–IRMS) system consisting of an Agilent HP 6890 gas chromatograph connected to a Finnigan Delta^{plus} XP isotope ratio mass spectrometer with a combustion interface. Gaseous compounds were separated on a HP-PLOT column (32 m × 0.32 mm i.d. × 10 μm), using an appropriate temperature program (40 °C for 2 min, 12 °C/min, 140 °C for 3 min). The NAUTINIL samples were analyzed only for stable carbon and hydrogen isotopes of hydrocarbon. The measurements were performed at Isolab BV using a Finnigan Delta S mass spectrometer connected to an Agilent HP 5890 gas chromatograph. Using a temperature program, gaseous compounds were separated on a molecular sieve (5 Å) PLOT column for methane and on a Porabond column for C_2–C_4 compounds. For corresponding samples, identical results were obtained for the two labs.

Data are reported in the usual δ notation: $\delta = \left(\frac{R_{sample}}{R_{standard}} - 1\right) \times 1000(‰)$, with R being the $^{13}C/^{12}C$ or the D/H ratio. The $\delta^{13}C$ values are given relative to the Vienna Peedee Formation belemnite (VPDB) and δD relative to the Vienna Standard Mean Ocean Water (VSMOW). For sediment samples, the average standard deviation for replicates was ±0.2‰ for $\delta^{13}C$ of methane and CO_2, ±0.5‰ for the C_{2+} gases, and ±2‰ for δD values. For water samples, due to lower gas concentrations, the average standard deviation was 0.5‰ for $\delta^{13}C$ of methane and ±2‰ for the C_{2+} hydrocarbons.

4.3.3. $\delta^{18}O$ and δD of pore fluids

Oxygen and hydrogen isotopic compositions were analyzed by modified standard techniques, using a mass spectrometer VG SIRA-24. Results are given in VSMOW. The precisions are 0.1‰ and 2‰ for the $\delta^{18}O$ and δD measurements, respectively. The detailed analytical procedure has been published elsewhere (Dählmann and de Lange, 2003).

4.3.4. Sulfate, chlorite, silicate, and phosphate measurements

Sulfate concentrations were measured on-shore as S from acidified and N_2-bubbled pore waters using ICP-AES. Chlorite concentrations were measured by

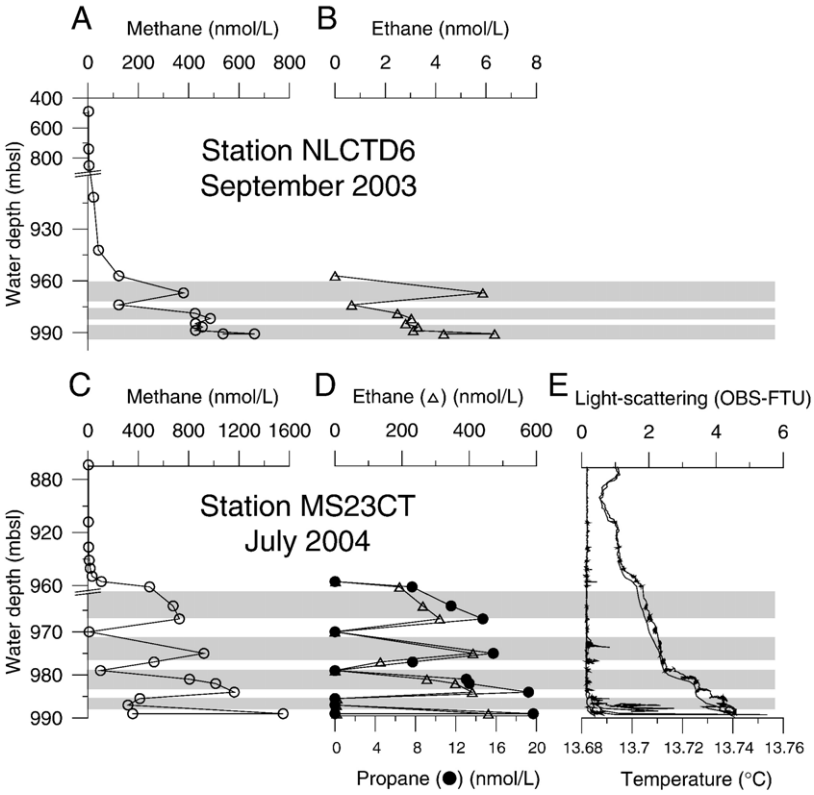

Fig. 2. Concentration of methane, ethane and propane, and temperature and light scattering profiles measured in the water column above Isis MV at stations NLCTD6 during NAUTINIL cruise (A and B) and at station MS23CT, during MIMES cruise (C–E). Note the breaks in the *y*-axes. The grey bands indicate the different sub-plumes.

potentiometric titration. For silicates and phosphates, all analyses were carried out on board on a TRAACS800 continuous flow analyzer, applying colorimetric methods after described by Grasshoff et al. (1983). The standard deviation for all measurements is 3% or better.

4.3.5. Temperature and light-scattering measurements

During the CTD casts, temperature was measured with an electronic thermometer part of the Conductivity–Temperature–Depth sensor (SeaBird SBE-9), and the light-scattering was measured by an optical backscatter meter (OBS).

5. Results

5.1. Water column

5.1.1. Molecular and isotopic composition of hydrocarbon gases

In 2004, during the MIMES cruise, a major enrichment of methane up to 1550 nmol/L occurred within 50 m above the seafloor at the Isis MV (Fig. 2C). These enrichments are well above the CH_4 of background value of seawater ($\sim^{1}$ nmol/L; Charlou et al., 2003). Besides the near bottom sub-plume, three additional sub-plumes are observed, with peak of methane concentration ranging from 730 to 1160 nmol/L (Fig. 2C). The concentration profiles of ethane (C_2) and propane (C_3) mimic that of methane (C_1) with concentrations in the deepest sample of 457 nmol/L and 20 nmol/L, respectively (Fig. 2D).

Similar, less distinct (possibly due to lower sample resolution) sub-plumes have been detected in 2003 during the NAUTINIL cruise (Fig. 2A and B). However, methane concentrations measured in 2004 are more than twice as high as those measured in 2003.

Stable carbon isotopic data of methane, ethane, and propane at MS23CT have variable values (Table 2). In the deepest sample, C_1, C_2, and C_3 components have $\delta^{13}C$ values of −53‰, −32‰, and −29‰, respectively. The heaviest $\delta^{13}C$ values for C_1–C_3 hydrocarbons, −12‰, −20‰, and −20‰, respectively, were measured at the top of the plume, i.e. at 961 m depth.

Table 2
Stable carbon isotopes of methane, ethane, propane and stable oxygen and hydrogen of water in the water column at station MS23CT (MIMES 2004 cruise)

Depth (mbsl)	$\delta^{13}C_1$ (‰)	$\delta^{13}C_2$ (‰)	$\delta^{13}C_3$ (‰)	δD (‰)	$\delta^{18}O$ (‰)
961	−12	−20	−20	5.2	1.2
967	−18	−25	−23	5.4	1.3
975	−47	−29	−27	6.5	0.9
977	−19	−21	n.d.	6.5	1.2
981	n.d.	−22	n.d.	5.6	1.2
984	−23	−20	−21	6.7	0.9
989	−53	−32	−29	7.0	1.2

n.d.: no data.
Isotopic data are given relative to VPDB for carbon and to VSMOW for hydrogen and oxygen (mbsl: meter below sea level).

5.1.2. Stable hydrogen and oxygen isotopic composition

In the water column, at station MS23CT, δD and $\delta^{18}O$ are constant in the whole sampling interval, with averaged values of 6.0‰ and 1.1‰ for δD and $\delta^{18}O$, respectively (Table 2).

5.1.3. Temperature and light-scattering

Down to 957 m, the seawater temperature remained constant (13.69 °C) and then, near the seafloor, steadily increased with increasing depth by up to 0.05 °C close to the seafloor (Fig. 2E). In the light-scattering profile, several peaks were noted between 960 and 989 m water depth, with a large plume detected approximately 10 m above the seafloor (Fig. 2E).

5.2. Sediment

Figs. 3A–H and 4A and D present results obtained from the sampling sites in the centre area. Figs. 3I–L (inset) and 4B and E show results obtained from sampling locations in the off-centre area. Since the aim of this study is to determine the origin of the gas, only the sedimentary gas samples between 130 and 600 cmbsf (centimeters below seafloor) will be discussed here. The sediments from 0–130 and >600 cmbsf are influenced by additional processes (e.g. oxidation) that will be discussed in detail elsewhere (Mastalerz et al., 2007).

5.2.1. Molecular composition of hydrocarbon gases

Measurements at the centre (stations NLK06F, MS09PC, MS19GT, and MS24PT, Fig. 3A) show high methane concentrations, up to 7500 µmol/L at 530 cmbsf, station MS09PC, well above those of the atmospheric equilibrium value of 0.9 mmol/L of wet sediment (given a methane solubility of 1.3 mmol/L at 22 °C and 1 bar pressure (Wiesenburg and Guinasso, 1979) and a sediment porosity of 0.7). Concurrently, sediments collected 220 m away from the centre of the Isis MV (MS11PT), show noticeably lower methane concentration (Fig. 3I). Further towards the edge of the MV in any direction (stations MS12PT, MS17PT, and MS13PT) the methane concentration decreases significantly (Figs. 3I and 5). Sediments collected 1 km away from the centre (MS13PT) show methane concentrations of a maximum of 0.7 µmol/L (Fig. 3I). Sediments from the reference site (MS22PT) taken >5 km away from the centre of the MV, exhibit methane concentrations of 0.2 µmol/L (Fig. 3I). Higher hydrocarbons (C_2 up to C_6) were only detected at stations from the centre area of the Isis MV but not from off-centre locations. Their abundance is here expressed as the wetness ratio (see also Section 3.1).

5.2.2. Stable carbon and hydrogen isotopic composition of hydrocarbon gases and CO_2

At the centre of the Isis MV, $\delta^{13}C$ and δD values of methane are relatively constant, and range from −56.5‰ to −55.3‰ (mean=−55.1‰) and from −180‰ to −212‰ (mean=−203‰), respectively (Fig. 3C and D). Stable carbon isotopes of ethane, propane, and *n*- and *i*-butane have also been measured at the centre (Fig. 3E, G, and H) and do not show significant variations with depth. The average $\delta^{13}C$ values are −30.3‰ for ethane, −26.1‰ for propane, −28.4‰ for *i*-butane, and −25.0‰ for *n*-butane. As the uppermost sedimentary intervals are influenced by diverse microbial processes (e.g. Figs. 3A, C and 4A; Mastalerz et al., 2007), we consider only the sedimentary section below ca. 130 cmbsf for the origin assessment towards the origin of hydrocarbons.

Compared to the centre stations, methane in the deepest samples at off-centre stations is relatively light in ^{13}C and heavy in D, namely $\delta^{13}C_1=-65‰$ at MS11PT, $\delta^{13}C_1=-78‰$ at MS17PT, and δD=−82‰ at MS11PT (Fig. 3K and L).

In the centre, a constant average $\delta^{13}C–CO_2$ value of −5.8‰ was measured in the lower sections of the cores during the MIMES cruise. At off-centre stations the carbon isotopic values for CO_2 are relatively light (−15.6‰, $n=12$), constant within the whole sediment sections, and similar to the values measured for the reference site (−17.9‰).

5.2.3. Pore water sulfate, silicate, and phosphate concentrations

At all sampling stations, the surface sulfate concentrations show values close to those of the seawater

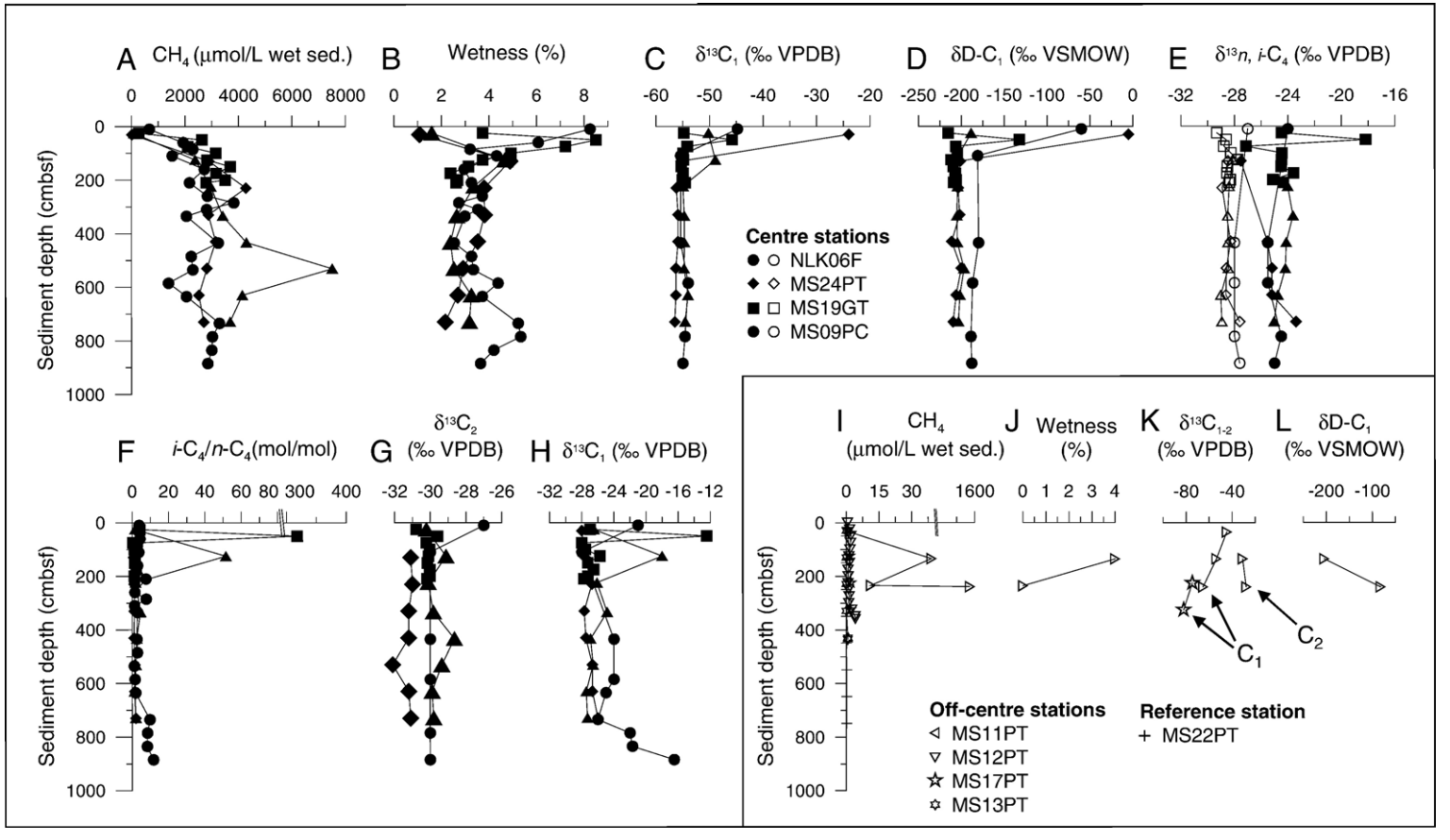

Fig. 3. At centre stations of Isis MV: methane concentration (A), wetness ratio (B), $\delta^{13}C$ and δD of methane (C, D), $\delta^{13}C$ of ethane (G), $\delta^{13}C$ of propane (H), $\delta^{13}C$ of butane (E; n-$^{C}_{4}$: filled symbols, i-$^{C}_{4}$: open symbols), and i-$^{C}_{4}$/n-$^{C}_{4}$ ratio (F). At off-centre of Isis MV (inset): methane concentrations (I), wetness ratio (J), $\delta^{13}C$ of methane and ethane (K), δD of methane (L). Isotopic data are given relative to VPDB for carbon isotope and VSMOW for hydrogen isotope. Note the break in x-axes of F and I.

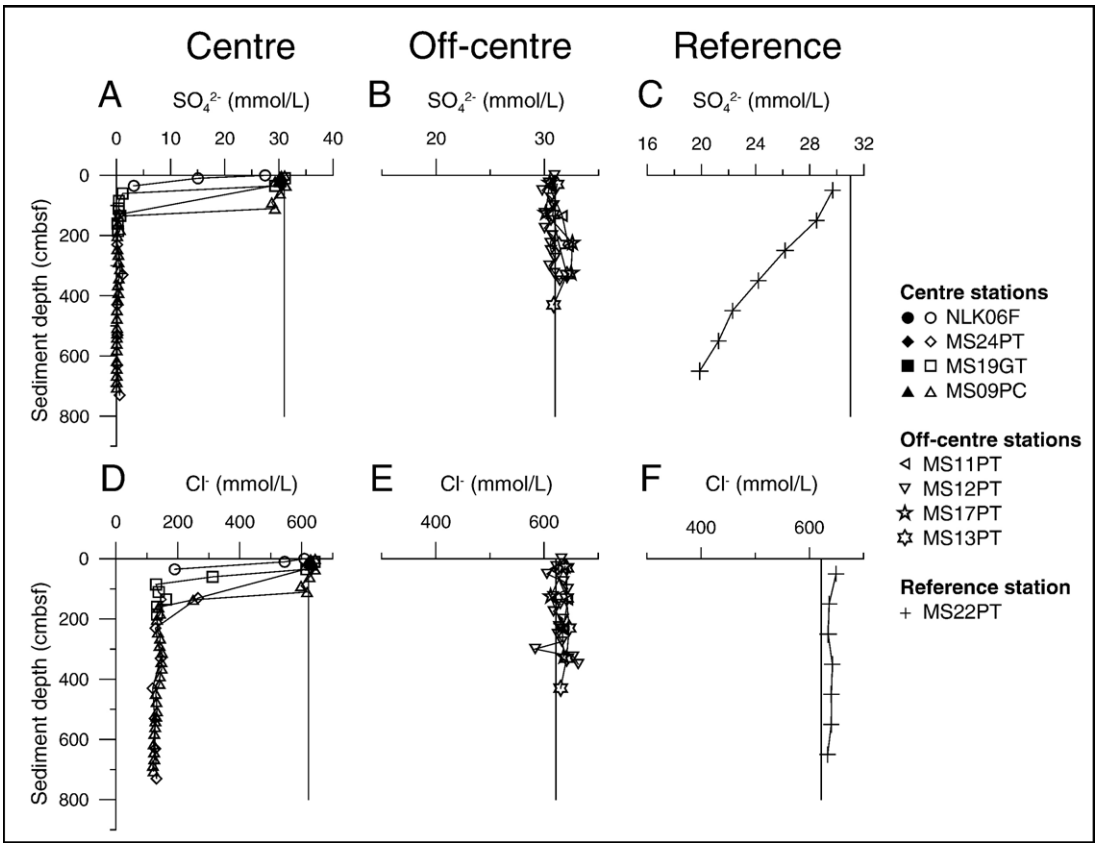

Fig. 4. Pore water concentrations of sulfate (A, B, C) and chlorite (D, E, F) at the centre, at the off-centre sites, and at the reference station. The straight lines refer to the bottom water concentration.

(Fig. 4A–C). At the reference station MS22PT, located outside the MV, the sulfate pore water distribution displays a smooth slightly curved profile (Fig. 4C), whereas, at the off-centre stations, sulfate remains at seawater concentration (Fig. 4B). At the centre, the sulfate concentrations display a more pronounced profile, with an estimated depth of zero sulfate concentration at 54 cmbsf for the station NLK06F (NAUTINIL) (Fig. 4A). During MIMES, central cores MS19GT and MS09PC were sub-sampled at higher resolution than MS24PT, which highlighted abrupt changes in the sulfate profiles (Fig. 4A). At MS19GT, within the upper 35 cm, sulfate remains at seawater concentration, but just below this depth the sulfate profile displays a dramatic kink and decreases to reach a sulfate concentration of 1.1 mmol/L at 60 cmbsf. A similar observation is made for MS09PC and MS24PT, but with sulfate depletion occurring below 125 cmbsf and 130 cmbsf, respectively.

All sediment sections from the off-centre locations display similar Si and PO_4 distribution patterns: low- and near-seawater values in the entire cored interval (Fig. 6B and E). In contrast, in the centre, the concentrations are at seawater values in the top meter and increase quickly downcore at concomitant of sulfate depletion, to reach values up to 24 μmol/L for $^{PO}_4$ and 300 μmol/L for Si (Fig. 6A and D). At the reference site, the Si and PO_4 profiles are concave in shape, typical for Mediterranean pelagic sediments, with concentrations increasing downward to reach values up to 11 μmol/L and 100 μmol/L, for PO_4 and Si, respectively (Fig. 6C and F).

5.2.4. Pore water chloride concentrations, and stable hydrogen and oxygen isotopic composition of pore water

At the reference station MS22PT, the chlorinity shows typical profile for Mediterranean pelagic sediments, with a constant concentration at bottom seawater value (Fig. 4F).

At the centre of the Isis MV and within the first meter section of the sediment column, not only chloride but also δD and δ^{18}O values of the pore fluid (620 mmol/L

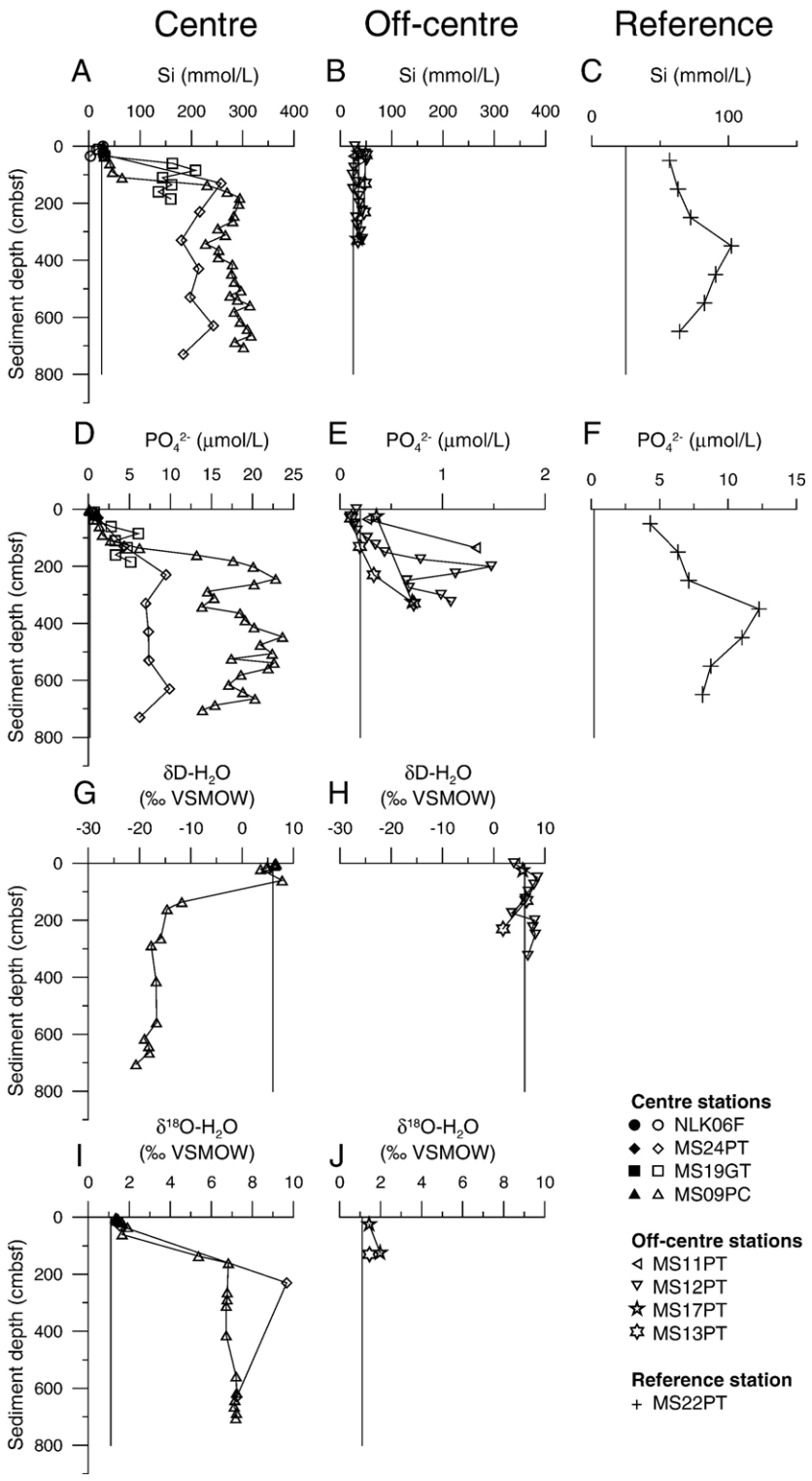

Fig. 5. Carbon isotopic ratio versus hydrogen isotopic ratio of methane [after Schoell (1988)]. Isotopic data are given relative to VPDB. The arrow "diffusion" indicates the processes that affect the isotopic composition of methane (see Section 6.1).

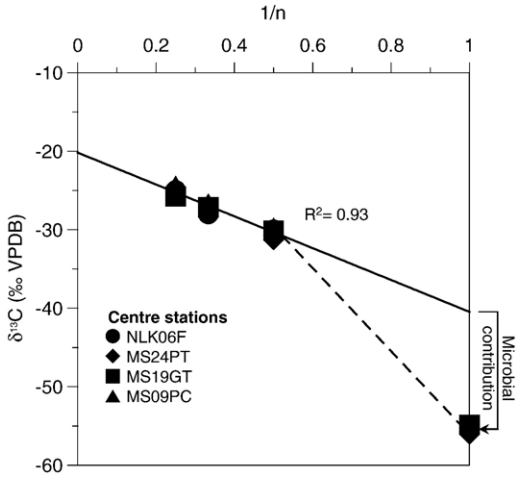

Fig. 6. Methane (CH_4, solid line) concentration and carbon isotopic ratio of methane ($\delta^{13}C_1$, dashed line) along a transect from the centre of the mud volcano to off-centre stations to the reference station. (Note the breaks in the *x*-axis and the left *y*-axis).

for Cl, 1.5‰ and 5.9‰ for $\delta^{18}O$ and δD, respectively) are similar to those of bottom Mediterranean seawater measured above the Isis MV (Figs. 4D, 6G and I and Table 2). Below this interval and deeper down the sediments, these values change dramatically to reach constant values for the rest the core (133 mmol/L for Cl, −17‰ and 7‰ for δD and $\delta^{18}O$, respectively).

At off-centre stations, the chloride concentration and isotopic composition of pore water remain at seawater values for the whole cored section (Figs. 4E and 6H, J).

6. Discussion

The obtained geochemical data set reveals three areas within the Isis MV which are characterized by different patterns of fluidodynamic: (1) the reference site 5.7 km away from the centre of the MV, (2) the off-centre region, and (3) the centre area (Fig. 1).

At the reference site, the concave-downward, decreasing sulfate concentration profile and a concomitant downward increasing phosphate profile is attributed to sulfate reduction and associated organic matter degradation processes (Figs. 4C and 6F; Borowski et al., 1999).

At the off-centre area, methane concentrations are low, and sulfate and silicate concentration gradients are absent (Figs. 3I, 4B, and 6B). These sediments thus show little evidence of organic matter degradation.

At the centre area of the MV, steep sulfate gradients (up to 112.8 mmol/L m^{-1}, station MS19GT, Fig. 4A) and silicate gradients associated with high gas concentrations suggest a strong upward advection of gas-enriched deep fluids (Figs. 3A, 4A, and 6A; Borowski et al., 1996; Aloisi et al., 2004). Moreover, the low-chlorinity of the deep pore fluid and its isotopic composition resulting from clay mineral dehydration (Cl = 133 mmol/L, δD–H_2O = −18‰, $\delta^{18}O$–H_2O = 7‰, Figs. 4D and 6G, I; see also Dählmann and de Lange, 2003) indicates not only a deep origin but also creates a density gradient and thus contributes as a driving force for gas-enriched, upward fluid advection (Henry et al., 1996).

6.1. Origin of the hydrocarbon gases

Since advecting gases do not undergo isotopic fractionation (Chanton, 2005), the central area is the best to determine the initial source of hydrocarbons. The off-centre area appears to be influenced by other processes such as diffusion. Therefore we will first discuss the central area followed by the off-centre sites.

6.1.1. Centre area

To assess the origin of the gases, several approaches introduced in Section 3 are used here.

At central sampling stations, the wetness ratio of hydrocarbon gases is about 3.5% (Fig. 3B), and according to the classification of Schoell (1983), is probably resulting from an ad-mixture of gases. Fig. 7 shows that none of the hydrocarbon gases fall into one of the well defined gas-origin boxes (thermogenic and microbial), but all samples show values of a mixed biogenic and thermogenic gas. In the natural gas plot (Fig. 8), the deviation of the $\delta^{13}C_1$ values from the C_2–C_4 isotope line supports the microbial contribution of isotopically light methane to the gas mixture. The $\delta^{13}C$ value of the pure thermogenic methane generated with the wet components can be estimated by extrapolating this line to $n = 1$, i.e. CH_4 (Section3.2). The pure isotopic thermogenic is thus estimated at −41.4‰. The ad-mixture of biogenic and thermogenic methane can then be quantified using a simple isotope mixing model. Assuming a $\delta^{13}C$ value for pure biogenic methane produced in marine sediments (−80‰; Whiticar, 1999), the biogenic contribution is estimated to represent 36% of the total methane. Considering that the C_{2+} components represent 3.5% of the total hydrocarbon gas, the biogenic contribution represents 35% of the total gas mixture, which leads to an initial gas wetness ratio of 5.7%.

The deep samples from the central cores clearly show a progressive ^{13}C enrichment with increasing carbon number and a linearity of the C_2–C_4 regression lines ($R^2 = 0.93$, Fig. 8). This indicates that the higher hydrocarbon gases have not been microbially altered. In

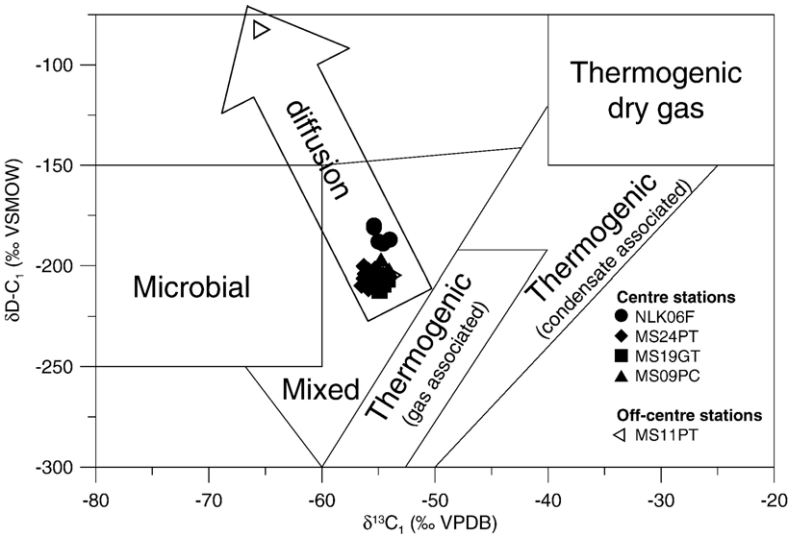

Fig. 7. Carbon isotopic ratio versus hydrogen isotopic ratio of methane (after Schoell, 1988). Isotopic data are given relative to VPDB. The arrow "diffusion" indicates the processes that affect the isotopic composition of methane (see Section 6.1).

addition, since straight-chain hydrocarbons are preferentially biodegraded relative to isoprenoidal hydrocarbons (Winters and William, 1969; Sassen et al., 1994), the relatively low i-C_4/n-C_4 ratio supports the absence of microbial degradation for these hydrocarbons (mean = 2.3 mol/mol, Fig. 3F). Accordingly, hydrocarbon gases collected from the centre area of the Isis MV show their mature characteristic.

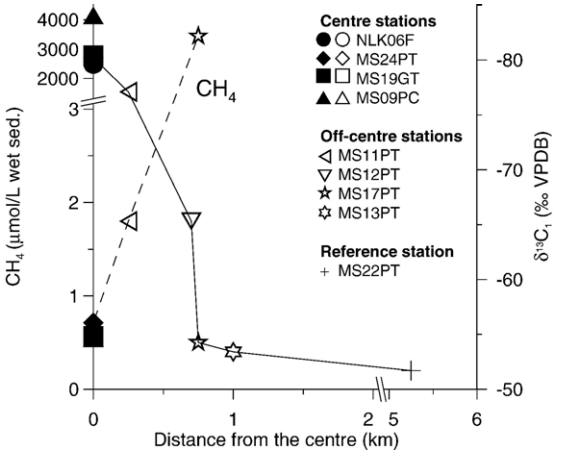

Fig. 8. "Natural gas plot model" according to Chung et al. (1988): reciprocal of the carbon chain length ($1/n$) versus the carbon isotopic ratio of the n-alkanes (dashed line). Isotopic data are given relative to VPDB. The average extrapolated C_2–C_4 regression line (solid line) has a correlation coefficient of 0.98. Extrapolation to $1/n = 0$ gives the $\delta^{13}C$ value of the source rock kerogen (−19.4‰); extrapolation to $1/n = 1$ gives the δC value of the thermogenic methane endmember (41.5‰). The deviation due to ad-mixture with microbial-produced methane is shown.

Fig. 9A shows the diagram established by Lorant et al. (1998). Studied samples fall in the secondary cracking zone with a corresponding vitrinite reflectance values ranging between 1.1% and 1.5%. This range corresponds to high maturity levels, indicating that the wet gases have been probably co-generated within the oil window (Hunt, 1996). This is also confirmed by the i-$C_4'$$n$-$C_4$ ratio which is consistent with a high source-rock maturity (Prinzhofer et al., 2000). This relatively wide maturity range suggests also mixing processes during migration. Nevertheless, the hydrocarbon gas data clearly indicate that the wet gases were generated within the oil window interval and confirm above estimations of (1) the $\delta^{13}C$ value obtained for the pure thermogenic methane (−41.5‰) and (2) the initial gas wetness ratio (5.7%). Both estimated values are also consistent with mature characteristics of the initial source rock (Hunt, 1996).

The natural gas plot can also be used to estimate the stable carbon isotopic signature of the source-rock kerogen. This value is determined by extrapolating the C_2–C_4 line to the y-axis, since the source can be approximated by molecules with an unlimited number of carbon atoms ($1/n \rightarrow 0$, Fig. 8; Chung et al., 1988). Doing so, a value of −19.4‰ is obtained. However, it was shown that the $\delta^{13}C$ intercept value is often higher than the actual $\delta^{13}C$ value of the kerogen, most likely due to heterogeneities of the source kerogen, to hydrocarbon formation mechanisms, or to maturity effects (Chung et al., 1988; Pohlman et al., 2005). In order to improve the estimated $\delta^{13}C$ value of the source kerogen, we use the empirical model developed by

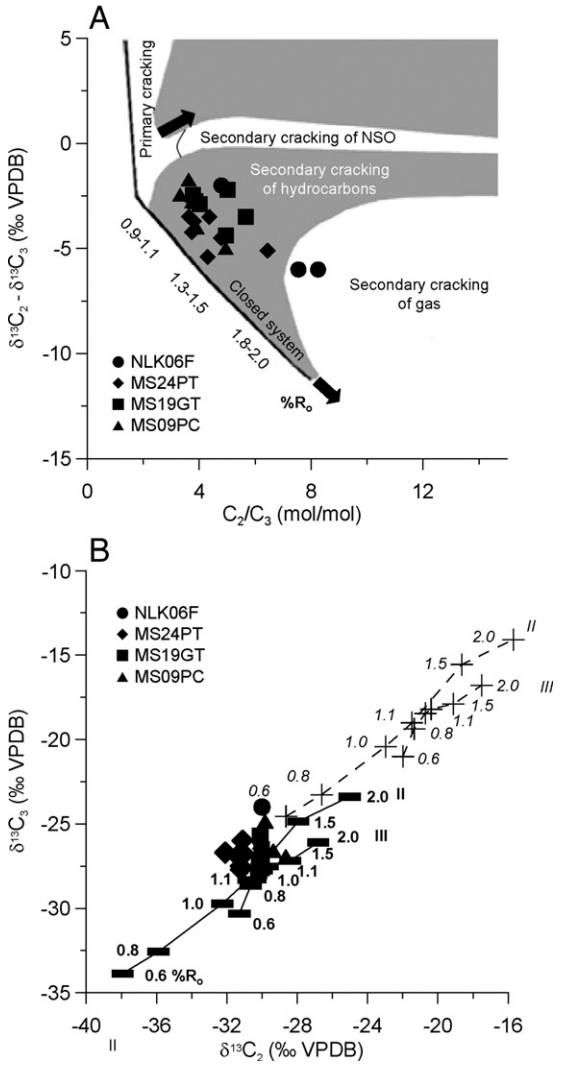

Fig. 9. (A) $^{C}_{2}/C_3$ ratio versus $\delta^{13}C_2$–$\delta^{13}C_3$ diagram (adapted from Lorant et al., 1998) from sampling sites in the center of Isis MV. (B) $\delta^{13}C_2$ versus C_3 diagram (after Berner and Faber, 1996). Isotopic data are given relative to VPDB. The maturity curves for type II and type III have been constructed using Appendix A and are for a $\delta^{13}C$ value of the source kerogen of −28.7‰ (solid lines, $\%R_o$ in normal font) and of −19.4‰ (obtained from the gas plot model, Fig. 8, dashed lines, $\%R_o$ in italic font). In both figures, vitrinite reflectance equivalent values are indicated along the maturity curves.

Berner and Faber (1996) (Section 3.3). Fig. 9B shows a $\delta^{13}C_2$ versus $\delta^{13}C_3$ diagram with the two maturity curves for kerogen type II and the kerogen type III. Since the kerogen $\delta^{13}C$ value has to be incorporated into the maturity equations (Appendix A, Eqs. (A.1)–(A.4)), we implemented it in the way to obtain the best fit with the estimated maturity range (1.1–1.5%, Fig. 9A). The maturity curves with the implemented $\delta^{13}C$ value of kerogen (−19.4‰) obtained from the gas plot model do not fit with the vitrinite reflectance range obtained above (Fig. 9B). This confirms the limit of the gas plot model of Chung et al. (1988) as a method for the approximation of the $\delta^{13}C$ signature for the original source rocks. In contrast, the equation of the type II kerogen shows better fit, with a kerogen $\delta^{13}C$ value of ca. −29‰ (Fig. 9B). This indicates that the C_{2+} hydrocarbons originate predominantly from a type II kerogen source, which is typical for marine environments. However, some contribution of type III kerogen cannot be excluded.

Apart from interpreting the origin of the gas as a mixture of a biogenic and a thermogenic endmember, ^{13}C-depleted methane can also be the result of isotopic fractionation during diffusive migration. However, it is unlikely that such diffusive fractionation occurs along the migration path through the central channel because MVs are primarily driven by advection and this mechanism is not associated with isotopic fractionation (Chanton, 2005). Therefore, if diffusive fractionation had occurred, it must have taken place prior to the gas expulsion, possibly between the subsurface oil source rock and reservoir (Fig. 10). If diffusive fractionation were significant, this would result in a $\delta^{13}C_1$ value even lighter than −41.4‰, thus leading to an even larger thermogenic contribution to the gas accumulation.

All this evidence demonstrates that a gas mixture dominated by a thermogenic origin, but with a significant biogenic contribution, migrates upward along a narrow channel at the centre of the Isis MV. Stable carbon isotope-based models indicate that the C_{2+} hydrocarbon gases originate predominantly from type II kerogen and are at the base of the central gas accumulation and expulsion.

6.1.2. Off-centre area

The molecular composition and concentration of hydrocarbon gas in the sediments from the off-centre area are significantly different compared to those at central locations. The gas is indeed relatively dryer (Fig. 3J) and the C_{2+} gaseous components are at very low concentration levels. Such difference in the molecular composition could be explained by either principally different sources for the hydrocarbon gases or by principally different fluid transfer mechanisms, which subsequently induced complex alterations in the migrated gas mixture.

Moreover, the constant seawater-like sulfate concentrations versus depth in off-centre sediments suggest a lack of upward fluid advection and of bacterial sulfate reduction processes (Fig. 4B). Consequently, the very low C_{2+} concentration, the absence of sulfate reduction and the relatively light $\delta^{13}C$ for CH_4 imply that methane from these sediments is likely diffused allochthonous gas and is not in-situ generated (Figs. 3K and 4B). There

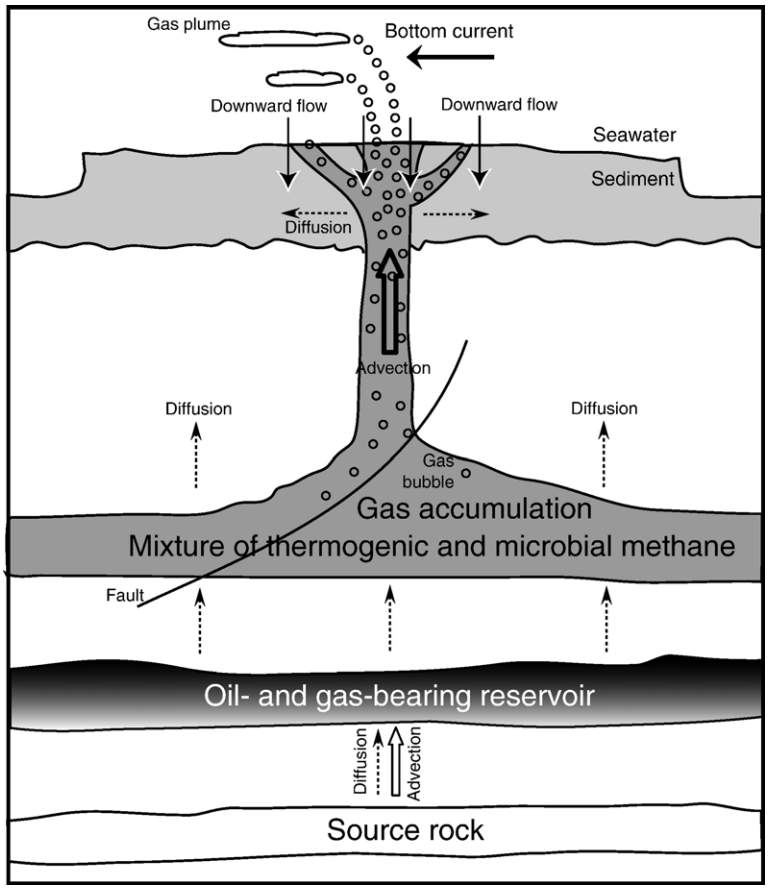

Fig. 10. Schematic representation (not to scale) of the migration pathways of hydrocarbons (modified after Kopf, 2002).

is a clear correlation between increasing distance from the centre, a decrease in the methane concentration and a shift towards negative $\delta^{13}C_1$ values (Fig. 5). In addition, the $\delta D–C_1$ value at the off-centre site MS11PT is 121‰ higher than for those at the centre (Fig. 3D and L). The shift in $\delta D–C_1$ being 12 times higher than the shift in $\delta^{13}C_1$ (10‰, Fig. 7) corresponds to results from experimental and natural observations on methane diffusion. The latter have indeed been reported as having a shift in $\delta D–C_1$ between 10 to 30 times larger than the shift in $\delta^{13}C_1$ (Fuex, 1980; Pernaton et al., 1996; Kittel, 1996). Our observations are therefore concordant with diffusion-related alterations from the initial isotopic composition as found in the centre, towards values encountered in the deepest samples at off-centre stations. Additionally, in off-centre sediments of MS11PT, the deepest sample exhibits a low ethane concentration and a $\delta^{13}C_2$ value similar to that measured at the centre (Fig. 3J and K). This result also argues for gas diffusion since the isotopic signature for ethane is not altered during diffusion (Zhang and Krooss, 2001; Lückge et al., 2002).

Finally, as to the molecular composition of C_{2+} hydrocarbon gases, Coleman et al. (1977) showed that migrated gas may be completely depleted of C_{2+} hydrocarbons. Besides, gas leakage through relatively impermeable and fluidized sediments can result in segregation of C_{2+} compounds (Schoell, 1983), which supports the low wetness ratio obtained in off-centre sediments as a result of methane diffusion occurring across the MV.

In summary, at off-centre stations, the carbon and hydrogen isotopic composition of methane measurable only in the deepest sediments indicates that it originates by diffusion from the same hydrocarbon source as that of the central area.

6.2. Pulses of gas injection into the water column by gas bubble transport

Gas concentrations and light-scattering profiles obtained during CTD casts show clear enhancements above the seafloor (Fig. 2A–E). Despite our careful sampling technique, such enhancements could potentially result from seafloor disturbance by the CTD-equipment.

If so, we would expect all sub-plumes to have (1) similar hydrocarbon isotopic compositions and (2) hydrocarbon isotopic composition close to that from the surface sediments. In contrast, the individual sub-plumes are largely different, with consistent gas isotopic compositions within each plume, but differing between them. Moreover, for each of the two CTD casts, the deepest two water samples have significantly different total hydrocarbon gas concentrations, despite being at the same water depth (Fig. 2A and C). The difference between the two samples at MS23CT is about 1200 nmol/L, although the two samples have been taken within a time interval of 13 s. These differences might be explained by lateral current which displaces the gas plume. Therefore, any gas release from sediment disturbance would have been "rapidly" removed compared to the sampling time of the CTD casts (33 min during NAUTINIL and 37 min during MIMES). Although some bottom disturbance by the bottom weight ~ 5 m below the CTD rosette cannot be entirely ruled out, the implemented delay prior to sampling and the considerations made above are convincing evidence that gas concentrations and light-scattering distributions observed above the Isis MV are "natural" profiles.

The sub-plumes observed above the Isis MV during the 2003 NAUTINIL cruise (Fig. 2A and B) show that substantial amounts of methane and ethane are introduced into the water column. During MIMES cruise in 2004, significant increases in the hydrocarbon concentrations were measured (Fig. 2C and D). This suggests an enhancement of the venting activity over this one year period. These hydrocarbon-rich sub-plumes are characteristic features of active gas venting, which emphasizes that MVs are significant geological source of hydrocarbons into the water column (Dimitrov, 2003). Furthermore, both CTD casts display identical distribution patterns for methane, ethane, and propane, which indicate that these gases have a common origin and are co-emitted into the water column. The light-scattering profile at MS32CT indicates that this gas discharge is associated with an emission of turbid fluids and/or bubble releases, which is also supported by the slight increase in temperature noted at the bottom of the plume (Fig. 2E).

Our gas profiles differ from those usually observed at MVs and gas seepages, where the CH_4 concentration often increases regularly with depth and well defined methane anomaly occurs right above the seafloor (Charlou et al., 2003). Water column gas plumes can also be the result of dissociation of gas hydrate fragments leaving the seafloor, rising in the water column and releasing methane locally (Suess et al., 1999; Charlou et al., 2004). This situation is inappropriate to our setting since the Isis MV is located outside the gas hydrate stability zone (bottom water temperature = 13.7 °C, pressure = 97.2 bar, salinity = 38.7‰; Sloan, 1989). The observed sub-plumes rather result from pulses of gas injections into the water column followed by mixing with seawater and lateral transport by bottom currents that may create distinct sub-plumes at different depth levels (Radlinski and Zbigniew, 1995). Stable carbon isotopic composition of methane, ethane, and propane may then serve as good natural tracers for gas injection. At MS23CT and in the sub-plumes at 989 and 975 mbsf, the $\delta^{13}C$ values of methane, ethane, and propane are similar to those measured in the deeper sediments at the centre of the MV (Fig. 3C, G, and H, and Table 2). The presence of sub-plumes above the Isis MV is therefore likely the result of gas injection pulses from a deep subsurface directly into the water column. Such unaltered gas inputs imply a gas bubble transport mechanism, because gas bubbles are not readily metabolized by microorganisms (Grant and Whiticar, 2002). Although no continuous bubble flows have been observed during the three *Nautile* dives, bubble saturation apparently occurs just beneath the sediment surface, as bubbles were released once the sediment surface was disturbed by the arm of the submersible (NAUTINIL cruise report). Bubble releases have also been recently observed at other MVs (Sauter et al., 2006; Greinert et al., 2006). In addition, seafloor observations at Hydrate Ridge showed that gas venting can occur intermittently with intervals of days to weeks (Tryon et al., 1999). Furthermore, during MIMES, acoustic gas plumes were detected in the water column, in particular above the centre of the Isis MV (Dupré et al., 2007). These acoustic observations are consistent with a gas bubble transport mechanism.

6.3. Driving forces and associated downward advection of bottom seawater

In the following sections we discuss first the centre area and then the off-centre area.

6.3.1. Centre area

In sediments, methane and sulfate are strongly reactive, such as in the microbially mediated process of anaerobic oxidation of methane or in the process of organic matter degradation (Reeburgh, 1982). The former process often leads to a SO_4 concentration decreasing linearly with depth in the sediment (e.g. Borowski et al., 1996), as observed for the station NLK06F at the centre of the Isis MV (Fig. 4A). However, the sulfate profile obtained at the same location but one

year later during the MIMES cruise has a kink-type profile with a conspicuously constant sulfate content for the uppermost meter (Fig. 4A, stations labelled MS). Although bioirrigation by tube dwelling organisms can also lead to an exchange of pore fluids with the overlying seawater (Emerson et al., 1984; Wallmann et al., 1997) this process is considered to be minor in this setting as no epifauna has been observed within the centre of the MV. Furthermore, bioirrigation alone cannot explain the observed rapid change in pore water profiles within 1 year and the constant seawater composition down to 125 cmbsf (Fig. 4A and D).

This clearly suggest that a non-steady state event occurred between the two cruises, which could either be (1) a recent mud flow mixed with seawater and/or (2) a downward advection of bottom seawater following a gas outburst.

6.3.1.1. Recent mud flow deposit followed by bottom water invasion. A mud flow deposit intimately mixed with bottom water can indeed lead to kink-type pore water SO_4 profiles (e.g. Hensen et al., 2003). In that case, turbulent mixing with bottom water during transport has resulted in a seawater composition of the mudflow pore water after deposition. Such intimate mixing is very unlikely in view of the potential ultimate ~100 m distance from any anticipated active mud eruption site at the centre of the Isis MV. Mud flow deposition followed by downward diffusion of bottom water is also unlikely as this would result in much more diffuse pore water concentration profiles and cannot explain the sharp depletion at 125 cmbsf and the fully seawater $\delta^{18}O$ and δD isotopic values for the pore water above this kink (Figs. 4A, D and 6G, I).

An alternative process that can explain isotopic and concentration profiles is downward advection of seawater following a recent gas expulsion, as it has also been suggested at other MVs (O'Hara et al., 1995; Henry et al., 1996). At the centre of the Isis MV, a bubble transport mechanism has been highlighted (Section 6.2). During bubble release, a downward influx of bottom seawater can be induced (Fossing et al., 2000; Kopf, 2002), resulting in important concave-down pore water profiles, as observed in the SO_4, Cl, and the Si profiles in the MIMES cores (Figs. 4A, D and 6A). Such process also concords with the isotopic composition of the pore water fluid that indicates a full bottom seawater signature in the whole uppermost sediment section (Fig. 6G and I). Hence, subsequent to each pulse of gas release is a phase of downward advection of bottom water until a next episode of mud expulsion occurs. The strength of such pulse, its gas contents, and the time interval between pulse and coring in particular, determine the depth of downward seawater progression. This process seems to control pore water dynamics at the centre of the Isis MV in accordance with the observed pore water profiles from 2003 and 2004 (Figs. 4 and 6), and is thought to be an important process for intermittently active mud expulsion systems elsewhere. An additional factor at the Isis MV may be the downward progression of bottom water which has a higher chlorinity and density than that of the ascending fluid (610 mmol/L versus 130 mmol/L, Fig. 4D and E, and 1.030 versus 1.007 kg/L).

An alternative process that can explain both isotopic and concentration data profiles is downward advection of seawater posterior to a recent gas expulsion. At the centre of the Isis MV, a bubble transport mechanism has been highlighted (Section 6.2). During bubble ebullition, a downward influx of bottom seawater can be induced, resulting in uppermost concave-down pore water portions, as observed in the SO_4, Cl, and the Si profiles in the MIMES cores (Figs. 4A, D and 6A). This is also in agreement with the isotopic composition of the pore water fluid that clearly shows a bottom seawater signature in the uppermost sediment section (Fig. 6G and I). Hence, subsequent to each pulse of gas release is a phase of downward advection of higher density bottom water until the next episode of fluid venting activity occurs. The intensity of such pulse, its gas contents, and the duration of the intermediate period all together determine the deepness of seawater penetration.

As shown at other MVs and in accordance with the observed pore water profiles during 2003 and 2004, downward advection of bottom seawater occurring straight after a gas expulsion seems the most feasible fluidodynamic process occurring at the centre of the Isis MV.

6.3.2. Off-centre area

At the off-centre area, downward advection of bottom seawater seems also to occur. Despite the presence of allochthonous methane originating from diffusion and the occurrence of some organic matter degradation as suggested by the increase with depth of dissolved phosphate and the relatively light $\delta^{13}C$ value for CO_2 similar to that found at the reference site (Section 5.2.2), constant seawater sulfate versus depth is observed for all cored intervals, down to 430 cmbsf (Figs. 4B and 6E). Moreover, the pore fluid isotopic composition for all off-centre sediments indicates a full seawater source, which rules out a deep fluid source contribution. Therefore, downward advection of seawater must even be more advanced for off-centre sediments. The influx might also be facilitated by the relatively high porosity of the

extruded mud (57%, NLK06F), which is consistent with the camembert-like morphology of the Isis MV thought to be characteristic for high porosity muds (Kopf, 2002). In view of the pore water data, and in particular its oxygen and hydrogen isotopic composition, a downward advection process of bottom water is clearly not only occurring in the centre but also in the off-centre areas of the Isis MV. Such downward advection of seawater can be directly related to gas expulsion at off-centre sites – as described above for the centre area – or could indirectly be related to gas expulsion at the centre area. Gas expulsion at the centre is associated with a compensational influx at off-centre sites, as observed at several venting sites around the world (Henry et al., 1996; Aloisi et al., 2004; Schmidt et al., 2005). Without direct observations of fluid flow measurements in the sediments, it is not possible to unambiguously discriminate between these two options for the centre. However, some circumstantial evidence is available. Active gas expulsion at off-centre sites is not only supported by acoustic observations during the MIMES cruise suggesting gas bubble release at the eastern and northern edges of the MV (Dupré et al., 2007) but also by the presence of black patches at off-centre sites as observed during the NAUTINIL cruise (NAUTINIL cruise report; Dupré et al., 2007). These black patches are characteristic of sulfide-rich, reduced sediments and may relate to recent methane emissions. In addition, it is hard to see that such convection cell mechanism alone could explain the presence of downward flow even at 450 m away from the centre of the mud structure (Station MS17PT, Fig. 1). It seems therefore that the most likely mechanism also for off-centre sites is gas eruption followed by downward advection of seawater. The off-centre gas releases must, however, occur at a much lower frequency when compared to the centre, thus leading to a much deeper progression of seawater.

6.4. Conceptual fluidodynamics within the Isis MV

Summarizing, we propose a model describing the gas and fluid migration pathways and the resulting associated processes at the Isis MV (Fig. 10). Gaseous hydrocarbons arriving from a deep reservoir migrate through the sediment column. During the migration, the hydrocarbon gases mix with microbial methane and partially accumulate within an appropriate lithological reservoir. Due to continuous transit of hydrocarbons from the source rock to this reservoir, overpressure develops. This growing overpressure eventually results in the outburst of fluid-saturated mud and a transient pulsed migration of gas. Depending on the oversaturation, these gases can form gas bubbles which potentially emanate into the water column, forming the plumes observed above the MV. Eruptions occur more frequently at the centre of the MV and more intermittently at the off-centre area. Following each gas outburst, downward inflow of overlying seawater is occurs. Because there is a shorter intermittent period between eruptive events due to higher and more continuous gas and fluids release dynamics, the bottom water inflow is shallower at the centre than at the off-centre area. To the best of our knowledge, this is the first time that such deep downward advection of bottom water is inferred for a MV environment.

7. Conclusions

A combination of geochemical tools used for hydrocarbon gas and pore water geochemistry was for the first time applied to the sediments and overlying water column to detect sources of ascending fluids and to reveal post-eruptional fluidodynamic processes.

The obtained data reveal that active gas venting occurs mainly at the very centre of the Isis MV, which results in high hydrocarbon gas concentrations in the sediments and in the overlying water column. The origin of these gases is largely thermogenic, as revealed by their stable carbon and hydrogen isotopes. These isotopic data also show that these gases were formed within the oil window interval, perhaps together with petroleum. The kerogen type established for the hydrocarbon gas likely belongs to the type II and is associated with sediments of various maturity levels.

Subsequent to each gas and fluid expulsion, downward advection of bottom water occurs, as suggested by the distinct kink in pore water dissolved species and hydrogen and oxygen isotopic profiles indicating a pure seawater signature above this kink. This process remains more shallow in the sediments at the centre area than at the off-centre zone, due to a higher frequency of gas outbursts at the centre. The transient charging and discharging of subsurface-accumulated gas and fluid is thought to be the driving force for pulses of gas release at the Isis MV.

MVs are a significant geological source of hydrocarbons and must incontestably be integrated into the global hydrocarbon budget. High resolution pore water and sediment sampling is essential to better understand the functioning of such mud structures; further studies will have to investigate not only the restricted active centre, but also the off-centre area in more detail.

Acknowledgements

We thank captains and crew-members aboard the R/V *Atalante* and *Pelagia* and the submersible *Nautile* for

their helpful assistance at sea, and all participants to NAUTINIL (chief scientist: J.-P. Foucher) and MIMES (chief scientist: J. M. Woodside) cruises for their collaboration. On-board technical assistance by L. Wuis, S. Asjes, and M. Laan from NIOZ-Texel were highly appreciated. We are also grateful for the laboratory work realized by R. Knoop, S. Gusic, B. van Os, K. Reimer, and A. van Dijk at Utrecht University, R. Kreulen and S. Welledonker at Isolab BV, and S. Verdegaal at the Free University, Amsterdam. A. Dale is acknowledged for his constructive comments on an earlier version of this manuscript, and A. Stadniskaia and W. Borowski for their constructive and valuable review that helped to improve the manuscript.

This work is supported by the EUROMARGINS Programme of the European Science Foundation and the Netherlands Organisation for Scientific Research (NWO project number 855.01.032, MEDIFLUX project).

Appendix A

Maturity equations corrected for the carbon isotopic composition of the source kerogen (δ^{13}C-kerogen) used in this study (Berner and Faber, 1996):

Type II kerogen:

$$\begin{aligned}\delta^{13}C - C_2 = {} & 7.4991(\%R_o)^6 - 81.906(\%R_o)^5 \\ & + 354.73(\%R_o)^4 - 772.76(\%R_o)^3 \\ & + 881.75(\%R_o)^2 - 482.97(\%R_o) \\ & + 60.083 + 30 - \delta^{13}C - \text{kerogen}\end{aligned} \quad (A.1)$$

$$\begin{aligned}\delta^{13}C - C_3 = {} & -2.0174(\%R_o)^6 + 8.294(\%R_o)^5 \\ & + 14.76(\%R_o)^4 - 126.87(\%R_o)^3 \\ & + 236.04(\%R_o)^2 - 165.11(\%R_o) \\ & + 3.87530 + 30 + \delta^{13}C - \text{kerogen}\end{aligned} \quad (A.2)$$

Type III kerogen:

$$\begin{aligned}\delta^{13}C - C_2 = {} & 3.198(\%R_o) - 26.901 + 22.4 \\ & + \delta^{13}C - \text{kerogen}\end{aligned} \quad (A.3)$$

$$\begin{aligned}\delta^{13}C - C_3 = {} & 4.903(\%R_o)^3 - 21.033(\%R_o)^2 + 30.436(\%R_o) \\ & - 36.164 + 22.8 + \delta^{13}C - \text{kerogen}\end{aligned} \quad (A.4)$$

These equations led to the construction of the four maturity curves plotted in Fig. 9B for type II and type III kerogen with an implemented δ^{13}C-kerogen value of −19.4‰ and −28.7‰.

References

Aloisi, G., Drews, M., Wallmann, K., Bohrmann, G., 2004. Fluid expulsion from the Dvurechenskii mud volcano (Black Sea) — part I. Fluid sources and relevance to Li, B, Sr, I and dissolved inorganic nitrogen cycles. Earth Planet. Sci. Lett. 225, 347–363.

Berner, U., Faber, E., 1996. Empirical carbon isotope/maturity relationships for gases from algal kerogens and terrigenous organic matter, based on dry, open-system pyrolysis. Org. Geochem. 24, 947–955.

Borowski, W.S., Paull, C.K., Ussler III, W., 1996. Marine pore-water sulfate profiles indicate in situ methane flux from underlying gas hydrate. Geology 24, 655–658.

Borowski, W.S., Paull, C.K., Ussler III, W., 1999. Global and local variations of interstitial sulfate gradients in deep-water, continental margin sediments: sensitivity to underlying methane and gas hydrates. Mar. Geol. 159, 131–154.

Burger, R.L., Fulthorpe, C.S., Austin, J.J.A., 2001. Late Pleistocene channel incisions in the southern Eel River Basin, northern California: implications for tectonic vs. eustatic influences on shelf sedimentation patterns. Mar. Geol. 177, 317.

Camerlenghi, A., Cita, M.B., Della Vedova, B., Fusi, N., Mirabile, L., Pellis, G., 1995. Geophysical evidence of mud diapirism on the Mediterranean Ridge accretionary complex. Mar. Geophys. Res. 17, 115–141.

Chanton, J.P., 2005. The effect of gas transport on the isotope signature of methane in wetlands. Org. Geochem. 36, 753–768.

Charlou, J.L., Donval, J.P., Zitter, T., Roy, N., Jean-Baptiste, P., Foucher, J.P., Woodside, J., and the MEDINAUT Scientific Party, 2003. Evidence of methane venting and geochemistry of brines on mud volcanoes of the eastern Mediterranean Sea. Deep-Sea Res., Part 1, Oceanogr. Res. Pap. 50, 941–958.

Charlou, J.L., Donval, J.P., Fouquet, Y., Ondreas, H., Knoery, J., Cochonat, P., Levaché, D., Poirier, Y., Jean-Baptiste, P., Fourré, E., Chazallon, B., and the ZAIROV Leg 2 Scientific Party, 2004. Physical and chemical characterization of gas hydrates and associated methane plumes in the Congo–Angola Basin. Chem. Geol. 205, 405–425.

Chung, H.M., Gormly, J.R., Squires, R.M., 1988. Origin of gaseous hydrocarbons in subsurface environments: theoretical considerations of carbon isotope distribution. Chem. Geol. 71, 97–103.

Cita, M.B., Ivanov, M.K., Woodside, J.M., 1996. The Mediterranean Ridge diapiric belt. Mar. Geol. 132, 1–6.

Clayton, C.J., Hay, S.J., Baylis, S.A., Dipper, B., 1997. Alteration of natural gas during leakage from a North Sea salt diapir field. Mar. Geol. 137, 69–80.

Cline, J.D., Holmes, M.L., 1977. Submarine seepage of natural gas in Norton Sound. Science 198, 1149–1153.

Coleman, D.D., Lin, C., Keogh, R.A., 1977. Isotopic identification of leakage gas from underground storage reservoirs — a progress report, Illinois State Geological Survey. Ill. Petrol. 111, 1–10.

Dählmann, A., de Lange, G.J., 2003. Fluid–sediment interactions at Eastern Mediterranean mud volcanoes: a stable isotope study from ODP Leg 160. Earth Planet. Sci. Lett. 212, 377–391.

de Lange, G.J., 1992. Shipboard routine and pressure-filtration system for pore-water extraction from suboxic sediments. Mar. Geol. 109, 77–81.

Dimitrov, L.I., 2002. Mud volcanoes—the most important pathway for degassing deeply buried sediments. Earth-Sci. Rev. 59, 49–76.

Dimitrov, L.I., 2003. Mud volcanoes — a significant source of atmospheric methane. Geo-Mar. Lett. 23, 155–161.

Dupré, S., Woodside, J., Foucher, J.-P., de Lange, G., Mascle, J., Boetius, A., Mastalerz, V., Stadnitskaia, A., Ondreas, H., Huguen, C., Harmegnies, F., Gontharet, S., Loncke, L., Deville, E., Niemann, H., Omoregie, E., Olu-Le Roy, K., Fiala-Medioni, A., Dahlmann, A., Caprais, J.-C., Prinzhofer, A., Sibuet, M., Pierre, C., Damste, J.S., 2007. Seafloor geological studies above active gas chimneys off Egypt (Central Nile Deep Sea Fan). Deep-Sea Res., Part 1, Oceanogr. Res. Pap. 54, 1146–1172.

Emerson, S., Jahnke, R., Heggie, D., 1984. Sediment–water exchange in shallow estuarine sediments. J. Mar. Res. 42, 702–730.

Fossing, H., Ferdelman, T.G., Berg, P., 2000. Sulfate reduction and methane oxidation in continental margin sediments influenced by irrigation (South–East Atlantic off Namibia). Geochim. Cosmochim. Acta 64, 897–910.

Fuex, A.N., 1980. Experimental evidence against an appreciable isotopic fractionation of methane during migration. Phys. Chem. Earth 12, 725–732.

Gaedicke, C., Baranov, B.V., Obzhirov, A.I., Lelikov, E.P., Belykh, I.N., Basov, E.I., 1997. Seismic stratigraphy, BSR distribution, and venting of methane-rich fluids west off Paramushir and Onekotan Islands, northern Kurils. Mar. Geol. 136, 259–276.

Grant, N.J., Whiticar, M.J., 2002. Stable carbon isotopic evidence for methane oxidation in plumes above Hydrate Ridge, Cascadia Oregon Margin. Glob. Biogeochem. Cycles 16. doi:10.1029/2001GB001851.

Grasshoff, K., Ehrhardt, M., Kremling, K., 1983. Methods of seawater analysis. VCH, Weinheim. 419 pp.

Greinert, J., Artemov, Y., Egorov, V., De Batist, M., McGinnis, D., 2006. 1300-m-high rising bubbles from mud volcanoes at 2080 m in the Black Sea: hydroacoustic characteristics and temporal variability. Earth Planet. Sci. Lett. 244, 1–15.

Henry, P., Le Pichon, X., Lallement, S., Lance, S., Martin, J.B., Foucher, J.-P., Fiala-Médioni, A., Rostek, F., Guilhaumou, N., Pranal, V., Castrec, M., 1996. Fluid flow in and around a mud volcano field seaward of the Barbados accretionary wedge: results from Manon cruise. J. Geophys. Res. 101, 20297–20323.

Hensen, C., Zabel, M., Pfeifer, K., Schwenk, T., Kasten, S., Riedinger, N., Schulz, H.D., Boetius, A., 2003. Control of sulfate pore-water profiles by sedimentary events and the significance of anaerobic oxidation of methane for the burial of sulfur in marine sediments. Geochim. Cosmochim. Acta 67, 2631–2647.

Hovland, M., Gallagher, J.W., Clennell, M.B., Lekvam, K., 1997. Gas hydrate and free gas volumes in marine sediments: example from the Niger Delta front. Mar. Pet. Geol. 14, 245–255.

Hunt, J.M., 1996. Petroleum Geochemistry and Geology. W. H. Freeman and company, San Fransiscopp.

James, A.T., Burns, B.J., 1984. Microbial alteration of subsurface natural gas accumulations. Am. Assoc. Pet. Geol. Bull. 68, 957–960.

Judd, A.G., Hovland, M., Dimitrov, L.I., Garcia Gil, S., Jukes, V., 2002. The geological methane budget at Continental Margins and its influence on climate change. Geofluids 2, 109–126.

Katz, B.J., Narimanov, A., Huseinzadeh, R., 2002. Significance of microbial process in gases of the South Caspian basin. Mar. Pet. Geol. 19, 783–796.

Kittel, D., 1996. A method for processing absorbed methane stable isotope data from the near surface on fractionation. In: Schumacher, D., Abrams, M.A. (Eds.), Hydrocarbon migration and its near surface expression. AAAPG Memoire, pp. 319–336.

Kopf, A.J., 2002. Significance of mud volcanism. Rev. Geophys. 40, 1–52.

Kopf, A.J., Behrmann, J.H., 2000. Extrusion dynamics of mud volcanoes on the Mediterranean Ridge accretionary complex. In: Vendeville, B., Mart, Y., Vigneresse, J.-L. (Eds.), Salt, Shale, and Igneous Diapirs in and around Europe. . Special Publication. The Geological Society of London, London, pp. 169–204.

Loncke, L., 2002. Le Delta Profond du Nil: Structure et évolution depuis le Messinien. PhD Thesis, Université Pierre et Marie Curie (Paris 6), 180 pp.

Loncke, L., Mascle, J., Fanil Scientific, P., 2004. Mud volcanoes, gas chimneys, pockmarks and mounds in the Nile deep-sea fan (Eastern Mediterranean): geophysical evidences. Mar. Pet. Geol. 21, 669–689.

Lorant, F., Prinzhofer, A., Behar, F., Huc, A.-Y., 1998. Carbon isotopic and molecular constraints on the formation and the expulsion of thermogenic hydrocarbon gases. Chem. Geol. 147, 249–264.

Lückge, A., Kastner, M., Littke, R., Cramer, B., 2002. Hydrocarbon gas in the Costa Rica subduction zone: primary composition and post-genetic alternation. Org. Geochem. 33, 933–943.

Mascle, J., Zitter, T., Bellaiche, G., Droz, L., Gaullier, V., Loncke, L., 2001. The Nile deep sea fan: preliminary results from a swath bathymetry survey. Mar. Pet. Geol. 18, 471–477.

Mastalerz, et al., 2007. Submitted to Geochemica et Cosmochemica Acta.

Mazurenko, L.L., Soloviev, V.A., 2003. Worldwide distribution of deep-water fluid venting and potential occurrences of gas hydrate accumulations. Geo-Mar. Lett. 23, 162–176.

Obzhirov, A., Shakirov, R., Salyuk, A., Suess, E., Biebow, N., Salomatin, A., 2004. Relations between methane venting, geological structure and seismo-tectonics in the Okhotsk Sea. Geo-Mar. Lett. 135–139.

O'Hara, S.C.M., Dando, P.R., Schuster, U., Bennis, A., Boyle, J.D., Chui, F.T.W., Hatherell, T.V.J., Niven, S.J., Taylor, L.J., 1995. Gas seep induced interstitial water circulation: observations and environmental implications. Cont. Shelf Res. 15, 931–948.

Pallasser, R.J., 2000. Recognising biodegradation in gas/oil accumulations through the [delta]13C compositions of gas components. Org. Geochem. 31, 1363–1373.

Pepper, A.S., Corvi, P.J., 1995. Simple kinetic models of petroleum formation. Part I: oil and gas generation from kerogen. Mar. Pet. Geol. 12, 291–319.

Pernaton, E., Prinzhofer, A., Schneider, F., 1996. Reconsideration of methane isotope signature as a criterion for the genesis of natural gas. Revue IFP 51, 635–651.

Pohlman, J.W., Canuel, E.A., Chapman, N.R., Spence, G.D., Whiticar, M.J., Coffin, R.B., 2005. The origin of thermogenic gas hydrates on the northern Cascadia Margin as inferred from isotopic ($^{13}C/^{12}C$ and D/H) and molecular composition of hydrate and vent gas. Org. Geochem. 36, 703–716.

Prinzhofer, A., Pernaton, E., 1997. Isotopically light methane in natural gas: bacterial imprint or diffusive fractionation? Chem. Geol. 142, 193–200.

Prinzhofer, A., Mello, M.R., Takaki, T., 2000. Geochemical characterization of natural gases: a physical multivariable approach and its application in maturity and migration estimates. Am. Assoc. Pet. Geol. Bull. 84, 1152–1172.

Radlinski, A.P., Zbigniew, L., 1995. Formation of light-hydrocarbon anomalies in oceanic waters. Geology 23, 265–268.

Reeburgh, W.S., 1982. A major sink and flux control for methane in marine sediments: anaerobic consumption. In: Fanning, K., Manheim, F.T. (Eds.), Dynamic Environment of the Ocean Floor. Heath, Lexington, Massachussets, pp. 203–217.

Sandstrom, M.W., Meredith, D., Kaplan, I.R., 1983. Hydrocarbon geochemistry in surface sediments of the Alaskan outer continental

shelf. Part 2: Distribution of hydrocarbon gases. Am. Assoc. Pet. Geol. Bull. 67, 2047–2052.

Sassen, R., MacDonald, I.R., Requejo, A.G., Guinasso, N., 1994. Organic geochemistry of sediments from chemosynthetic communities, Gulf of Mexico slope. Geo-Mar. Lett. 14, 110–119.

Sassen, R., Joye, S., Sweet, S.T., DeFreitas, D.A., Milkov, A.V., MacDonald, I.R., 1999. Thermogenic gas hydrates and hydrocarbon gases in complex chemosynthetic communities, Gulf of Mexico continental slope. Org. Geochem. 30, 485–497.

Sauter, E.J., Muyakshin, S.I., Charlou, J.-L., Schluter, M., Boetius, A., Jerosch, K., Damm, E., Foucher, J.-P., Klages, M., 2006. Methane discharge from a deep-sea submarine mud volcano into the upper water column by gas hydrate-coated methane bubbles. Earth Planet. Sci. Lett. 243, 354–365.

Schmidt, M., Hensen, C., Morz, T., Muller, C., Grevemeyer, I., Wallmann, K., Mau, S., Kaul, N., 2005. Methane hydrate accumulation in "Mound 11" mud volcano, Costa Rica forearc. Mar. Geol. 216, 83–100.

Schoell, M., 1980. The hydrogen and carbon isotopic composition of methane from natural gases of various origins. Geochim. Cosmochim. Acta 44, 649–661.

Schoell, M., 1983. Genetic characterization of natural gases. Am. Assoc. Pet. Geol. Bull. 67, 2225–2238.

Schoell, M., 1988. Multiple origins of methane in the earth. Chem. Geol. 71, 1–10.

Shakirov, R., Obzhirov, A.I., Suess, E., Salyuk, A., Biebow, N., 2004. Mud volcanoes and gas vents in the Okhotsk Sea area. Geo-Mar. Lett. 24, 140–149.

Sherwood Lollar, B., Westgate, T.D., Ward, J.A., Slater, G.F., Lacrampe-Couloume, G., 2002. Abiogenic formation of alkanes in the Earth's crust as a minor source for global hydrocarbon reservoirs. Nature 416, 522.

Sloan, E.D., 1989. Clathrate Hydrates Of Natural Gases. Marcel Dekker Inc., New York. 641 pp.

Stahl, W.J., 1977. Carbon and nitrogen isotopes in hydrocarbon research and exploration. Chem. Geol. 20, 121–149.

Stahl, W.J., 1979. Carbon isotopes in petroleum geochemistry. In: Jäger, E., Hunziker, J.C. (Eds.), Lectures in isotopes geology. Springer-Verslag, pp. 274–282.

Suess, E., Bohrmann, G., von Huene, R., Peter, L., Wallman, K., Lammers, S., Sahling, H., 1998. Fluid venting in the eastern Aleutian subduction zone. J. Geophys. Res. 103, 2597–2614.

Suess, E., Torres, M.E., Bohrmann, G., Collier, R.W., Greinert, J., Linke, P., Rehder, G., Trehu, A., Wallmann, K., Winckler, G., Zuleger, E., 1999. Gas hydrate destabilization: enhanced dewatering, benthic material turnover and large methane plumes at the Cascadia convergent margin. Earth Planet. Sci. Lett. 170, 1–15.

Tryon, M.D., Brown, K.M., Torres, M.E., Trehu, A.M., McManus, J., Collier, R.W., 1999. Measurements of transience and downward fluid flow near episodic methane gas vents. Geology 27, 1075–1078.

von Rad, U., Berner, U., Delisle, G., Doose-Rolinski, H., Fechner, N., Linke, P., Roeser, H.A., Schmaljohann, R., Wiedicke, M., Parties, S.S., 2000. Gas and fluid venting at the Makran accretionary wedge off Pakistan. Geo-Mar. Lett. 20, 10–19.

Wallmann, K., Linke, P., Suess, E., Bohrmann, G., Sahling, H., Schlüter, M., Dählmann, A., Lammers, S., Greinert, J., von Mirbach, N., 1997. Quantifying fluid flow, solute mixing, and biogeochemical turnover at cold vents of the eastern Aleutian subduction zone. Geochim. Cosmochim. Acta 61, 5209–5219.

Whiticar, M.J., 1999. Carbon and hydrogen isotope systematics of microbial formation and oxidation of methane. Chem. Geol. 161, 291–314.

Wiesenburg, D.A., Guinasso Jr., N.L., 1979. Equilibrium solubilities of methane, carbon monoxide, and hydrogen in water and sea water. J. Chem. Eng. Data 24, 356–360.

Winters, J.C., William, J.A., 1969. Microbiological alteration of crude oil in the reservoir. Symposium on petroleum transformation in geologic environments, pp. E22–E31.

Woodside, J.M., Ivanov, M.K., Limonov, A.F., Shipboard Scientists of the ANAXIPROBE expeditions, 1998. Shallow gas and gas hydrates in the Anaximander Mountains region, eastern Mediterranean Sea. In: Henriet, J.-P., Mienert, J. (Eds.), Gas Hydrates — Relevance to World Margin Stability and Climate Change. Geological Society Special Publication. The Geological Society, London, pp. 177–193.

Zhang, T., Krooss, B.M., 2001. Experimental investigation on the carbon isotope fractionation of methane during gas migration by diffusion through sedimentary rocks at elevated temperature and pressure. Geochim. Cosmochim. Acta 65, 2723–2742.

Zitter, T., 2004. Mud volcanism and fluid emission in Eastern Mediterranean neotectonic zones. PhD Thesis, Vrije Universiteit, Amsterdam, 140 pp.